DEEP LEARNING TECHNIQUE TO DENOISE ELECTROMYOGRAM ARTIFACTS FROM SINGLE-CHANNEL ELECTROENCEPHALOGRAM SIGNALS

Muhammad E. H. Chowdhury[1], Md Shafayet Hossain[2], Sakib Mahmud[1] and Amith Khandakar[1]

[1]Department of Electrical Engineering, Qatar University, Doha, 2713, Qatar
[2]Department of Electrical, Electronic and Systems Engineering, Universiti Kebangsaan Malaysia, Bangi, 43600, Selangor, Malaysia

ABSTRACT

The adoption of dependable and robust techniques to remove electromyogram (EMG) artifacts from electroencephalogram (EEG) is essential to enable the exact identification of several neurological diseases. Even though many classical signal processing-based techniques have been used in the past and only a few deep-learning-based models have been proposed very recently, it is still a challenge to design an effective technique to eliminate EMG artifacts from EEG. In this work, deep learning (DL) techniques have been used to remove EMG artifacts from single-channel EEG data by employing four popular 1D convolutional neural network (CNN) models for signal synthesis. To train, validate, and test four CNN models, a semi-synthetic publicly accessible EEG dataset known as EEGdenoiseNet has been used the performance of 1D CNN models has been assessed by calculating the relative root mean squared error (RRMSE) in both the time and frequency domain, the temporal and spectral percentage reduction in EMG artifacts and the average power ratios between five EEG bands to whole spectra. The U-Net model outperformed the other three 1D CNN models in most cases in removing EMG artifacts from EEG achieving the highest temporal and spectral percentage reduction in EMG artifacts (90.01% and 95.49%); the closest average power ratio for theta, alpha, beta, and gamma band (0.55701, 0.12904, 0.07516, and 0.01822, respectively) compared to ground truth EEG (0.5429; 0.13225; 0.08214; 0.002146; and 0.02146, respectively). It is expected from the reported results that the proposed framework can be used for real-time EMG artifact reduction from multi-channel EEG data as well.

KEYWORDS

EEG, EMG artifacts, Deep Learning, Single Channel, Denoising, Convolutional neural network.

1. INTRODUCTION

An electroencephalogram (EEG) signal is recorded non-invasively at the scalp which represents electrical pulses originating from the brain's electrophysiological activity [1]. EEG is important for several therapeutic uses and in neurological research. EEG is mostly used to diagnose epileptic seizures and Alzheimer's disease in humans [2, 3]. Other applications of EEG include drowsiness level measurement [4], detection of human emotions [5], estimation of cognitive workload [6], brain-computer interfaces (BCIs) [7], and biometric systems [8].

David C. Wyld et al. (Eds): SIGEM, MLTEC, SEAPP, ITCON, NATL, FUZZY, CSEA - 2022
pp. 85-98, 2022. CS & IT - CSCP 2022 DOI: 10.5121/csit.2022.122006

EEG recordings are highly susceptible to physiological noises such as myogenic artifacts [9], ocular artifacts [10], cardiac abnormalities [11], and non-physiological disturbances like power line noise and motion artifacts [12]. These noises will have a big effect on how the EEG data is analyzed, and in the worst cases, they could even lead to a completely wrong clinical diagnosis. To reduce artifacts and keep as much of the neural information as possible, an efficient and robust framework is vital which can remove EMG artifacts from EEG data.

The Fourier transform or the wavelet transform was commonly used to translate the signal from the temporal domain to the spectral domain and then filter out the spectral components that correspond to the EMG artifacts. The EMG artifacts-free EEG signal can be obtained using either the inverse Fourier transform or the inverse wavelet transform. The use of Wiener filter [13], adaptive filter [14], Hilbert-Huang Transformation (HHT) [15], empirical mode decomposition (EMD) [16], variational mode decomposition (VMD) [17], independent component analysis (ICA) [18], and canonical correlation analysis (CCA) [19] etc. are some other methods for EEG denoising. These methods aimed to transform the signal from its original space to a new space where the signal and noise can be separated. Some of the major disadvantages of utilizing a signal-processing-based algorithm to remove EMG artifacts from EEG recordings are the low percentage reduction in EMG artifacts removal, high possibility of removing important neural information from EEG by considering artifacts components, poor performance in dynamic situations, etc. Extended EMD (EEMD)-ICA and EEMD-CCA [20, 21] are two hybrid approaches that were reported to remove EMG artifacts from EEG. Although the integration of ICA/CCA along with EMD/EEMD improved the performance to some extent, the underlying assumptions remained unclear and requires optimization through trial and error basis. As an example, in the EEMD-CCA, the choice of two autocorrelation criteria is experimentally determined in diverse circumstances [22].

The development of novel network topologies and learning methods, as well as the increase in computer resources and enormous data processing capacity, have significantly enhanced the performance of deep learning (DL) neural networks in recent years. Several technological problems, including image processing [23] and natural language processing [24], have been effectively solved using DL. The categorization of motor imagery based on EEG [25] and the reconstruction of EEG [26] are two notable applications of EEG-related analysis that make use of DL methods.

EEG artifacts have also been eliminated using certain well-known deep learning (DL) models, including auto-encoder [27], convolutional neural networks (CNNs) [28, 29], and recurrent neural networks [29, 30]. In comparison to conventional signal processing-based models, DL models have the following two advantages: (i) universality, where a standardized architecture can accommodate a variety of artifact removal tasks without the need for manual designs of prior assumptions on a particular type of artifacts; and (ii) higher capacity, where deep learning enforces a significant performance improvement. As expected, a significant performance boost compared to the traditional signal-processing-based methods was reported in these studies yet some of the shortcomings of these deep learning-based approaches are : testing the proposed models with a partial dataset rather than using the k-fold cross-validation approach, lack of generability of the model, room for a further performance boost, smaller number of performance metrics for evaluating the DL models, etc which are addressed properly in this study.

The goal of this study is to create an efficient and robust DL model that can clean out EMG artifacts from EMG-corrupted EEG data. To denoise EMG artifacts from contaminated EEG signals, four different 1D CNN models, namely (i) Feature Pyramid Network, or FPN [31], (ii) U-Net [32], (iii) Multi-level Context Gating U-Net (MCGU-Net) [33], and (iv) LinkNet [34] have been implemented in this work. The efficacy of the models is then compared by computing

several performance metrics, using the publicly available semi-synthetic dataset, EEGdenoiseNet. Our main contributions are listed here, briefly:

- The outcomes of our thorough analysis provide a convincing demonstration of the effectiveness of 1D CNN models in eliminating EMG artifacts from noisy EEG.
- The four 1D-CNN models are trained and tested using a five-fold cross-validation method and consistent results obtained from each fold ensure the reliability and robustness of the proposed framework.
- After being trained on single-channel, semi-synthetic EEG data, our created framework may be utilized to denoise multichannel, real-world EEG data.

The rest of this article is organized as follows: The single-channel EEG dataset, semi-synthetic corrupted EEG data creation, and normalization approaches used in this research are described in Section 2. The experimental setup and the performance assessment metrics are covered in Section 3. In Section 4, the performance of the proposed four different cutting-edge 1D CNN segmentation networks is quantified, and the findings are thoroughly discussed. The limitations of our research are described in Section 5 and finally, a succinct conclusion is presented in section 6.

2. MATERIALS AND METHODS

The framework for efficient EEG denoising (removing EMG artifacts from contaminated EEG) utilizing 1D-CNN-based segmentation networks is shown in **Figure 1** and is self-explanatory. In two distinct subsections, the dataset utilized, the semi-synthetic data creation, and the normalization processes employed in this work are elaborately explained below:

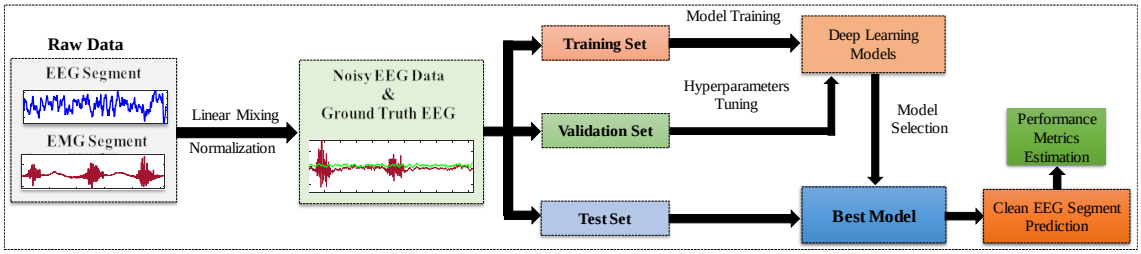

Figure 1. A proposed framework to remove EMG artifacts from corrupted EEG signals.

2.1. Dataset Description

The EEGdenoiseNet, a semi-synthetic EEG dataset is used in this study [29]. The noisy EEG and equivalent clean EEG provided by EEGdenoiseNet are used for model training and quantitative performance assessment. It may be used to assess how well different models generalize in real-world circumstances. The EEGdenoiseNet dataset includes 4,514 clean EEG signal segments and 5,598 clean EMG signal segments. Each clean EEG and EMG signal segment is 2 seconds long.

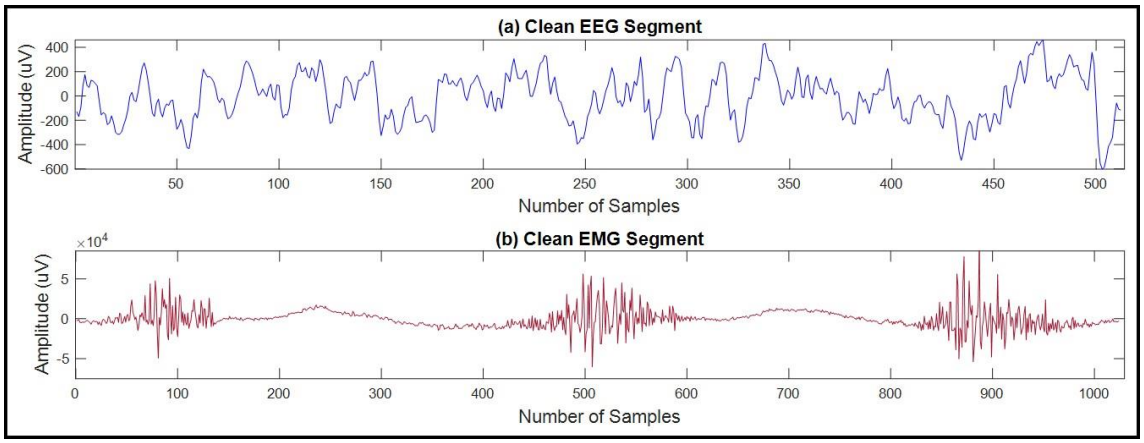

Figure 2. Example segments in EEGdenoiseNet dataset. (a) Clean/Ground truth EEG segment, (b) Clean EMG segment.

The raw EEG signals were pre-processed with a band-pass filter (1-80 Hz) to remove unnecessary high-frequency components of EEG, a notch filter (50 Hz) to remove the powerline noises, and re-sampled at 256 Hz by the authors of the dataset [29]. The EEG signals were segmented at this stage, with each segment containing 512 data points (2 seconds). It is important to note that single-channel EEG signals were used to construct the clean EEG segments. Raw face EMG signals were resampled to 512 Hz after being band-pass filtered (bandwidth: 1-120 Hz) and notch filtered at the power-line frequency (50 Hz). Because the EMG signal is concentrated in the high-frequency band, the EMG signals were sampled at 512 Hz instead of 256 Hz to preserve the high-frequency component of EMG signals. Finally, one-dimensional, 2-second EMG segments with 1024 data points per segment were generated. **Figure 2** depicts one clean EEG, and one clean EMG segment for visual illustration.

2.2. Semi-Synthetic Contaminated EEG Data Generation and Normalization

In this study, the clean EEG segments are linearly mixed with EMG segments (**Equation 1)** to produce the semi-synthetic EMG contaminated EEG:

$$y = x + \lambda.n \tag{1}$$

where x denotes the clean EEG segment/ground truth EEG; n is the clean EMG segment (as noise), and y is the semi-synthetic EMG contaminated EEG segment. The signal-to-noise ratio (SNR) of the EMG corrupted EEG signal can be varied by changing the value of the scaling factor λ by solving **Equation 2**:

$$SNR = 10log\frac{RMS(x)}{RMS(\lambda.n)} \tag{2}$$

The root mean square (RMS) can be calculated as follows:

$$RMS\,(z) = \sqrt{\frac{1}{N}\sum_{i=1}^{N} z_i^2} \tag{3}$$

where N is the number of time-domain samples of segment, z and z_i is the i_{th} sample point of segment, z. It is apparent from **Equation 2** that a smaller λ corresponds to lesser EMG artifacts and hence a lower λ indicates a higher SNR. Similarly, higher noise level results in poorer SNR.

The SNR of an EEG that has been contaminated by EMG artifacts typically ranges from -7dB to 2dB [35].

In this work, the linear mixing process enables us to generate a pair of EEG segments (x, y) where the clean/ground truth EEG (x) can be utilized as the outputs and the semi-synthetic EMG contaminated EEG (y) as the inputs to train the end-to-end deep learning models. However, in this study, (x, y) pairs are not directly fed to 1D CNN models. Rather, both the EMG contaminated EEG and ground truth EEG segments are divided by the standard deviation of the EMG contaminated EEG segments (σ_y) and the resultant **(Equation 4**) normalized segments $(\hat{x}, \hat{y})$ are utilized as inputs and outputs to facilitate the learning procedure of the deep learning models.

$$\hat{x} = \frac{x}{\sigma_y} \; ; \; \hat{y} = \frac{y}{\sigma_y} \tag{4}$$

4,514 clean EEG segments and 5,598 EMG segments are mixed while maintaining a particular SNR to produce the EMG-contaminated EEG segments. 4,514 clean EMG segments are chosen at random from a pool of 5,598 EMG segments to match the number of the EEG signal segments. Before combining EEG and EMG segments linearly, all the clean EEG segments are up-sampled at 512 Hz to match the sampling frequency of EMG segments. We repeat this procedure ten times for ten different SNR levels (-7 dB, -6 dB, -5 dB, -4 dB, -3 dB, -2 dB, -1 dB, 0 dB, 1 dB, and 2 dB), giving us 45,140 EMG-contaminated EEG segments. **Figure 3** shows a randomly selected (out of 45,140 segments) EMG contaminated EEG segment. In **Figure 3**, the corresponding ground truth EEG segment is also overlaid to better visualize the impact of EMG contamination in EEG.

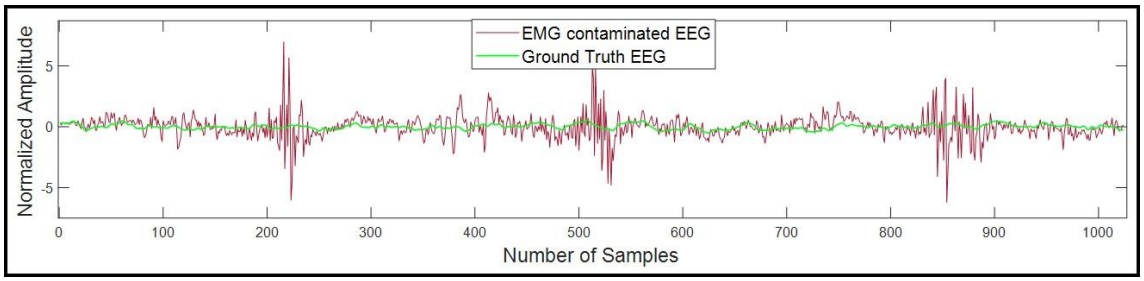

Figure 3. Example segments of EMG contaminated EEG and corresponding overlaid ground truth EEG.

3. EXPERIMENT DETAILS

The four 1D CNN models (FPN, U-Net, MCGU-Net, and LinkNet) are trained in an end-to-end framework, i.e., the normalized contaminated EEG segments $(\hat{y})$ are fed into the neural networks as input and corresponding ground truth EEG segments $(\hat{x})$ are fed as output so that the DL models can develop a nonlinear function that maps the contaminated EEG segments $(\hat{y})$ to the ground truth EEG segments $(\hat{x})$. During training, the mean squared error (MSE) is selected as the loss function, ADAM optimizer is applied to optimize the loss function. The learning rate α is set to 0.0005. The training set consists of 80% of the data, while the test set consists of the remaining 20%. The validation set is selected from the 10% of the training set. It is important to note that each EEG and EMG segment in the dataset is acquired from a distinct individual, hence the 80-20-10 splitting results in no data leakage across the train, test, and validation sets. In the Google ColabPro environment, the five-fold cross-validation approach is adopted to independently train, validate, and test all four networks separately. Two distinct experiments are conducted in this research and are explained below:

3.1. Experiment A

As previously mentioned, 4,514 EEG segments contaminated with EMG artifacts are created for each of the 10 SNR values (-7 dB, -6 dB, -5 dB, -4 dB, -3 dB, -2 dB, -1 dB, 0 dB, 1 dB, and 2 dB), yielding 45,140 EEG segments overall. The EMG-corrupted EEG and associated ground truth EEG segments are used to train each of the four 1D CNN models 10 times for a total of 10 distinct SNR values, separately. This means that at SNR level -7 dB, 80% of the 4,514 segments (3,611) are used as the training set, while the remaining 20% of the 4,514 segments (903) are used as the test set. Similarly, segments generated from nine more SNR levels (-6 dB, -5 dB, -4 dB, -3 dB, -2 dB, -1 dB, 0 dB, 1 dB, and 2 dB) are individually subjected to the same procedure, separately. Table 1 consists of the information for train and test sets formation.

Table 1. Formation of train and test sets for experiment B

SNR level (in dB)	Total Number of ground truth EEG and EMG contaminated EEG	Train set (80% of ground truth EEG and EMG contaminated EEG pairs)	Test set (20% of ground truth EEG and EMG contaminated EEG pairs)
-7	4,514	3,611	903
-6	4,514	3,611	903
-5	4,514	3,611	903
-4	4,514	3,611	903
-3	4,514	3,611	903
-2	4,514	3,611	903
-1	4,514	3,611	903
0	4,514	3,611	903
+1	4,514	3,611	903
+2	4,514	3,611	903

To assess the effectiveness of all four DL models in removing EMG noises from contaminated EEG, Deep Supervision [36] is applied, and three well-known performance metrics (correlation coefficient, relative root mean squared error in the time and frequency domain) are computed.

3.2. Experiment B

In the second experiment, the training and test sets are created in a more controlled setting. For each of the ten distinct SNR levels, eighty percent EMG corrupted EEG segments and their corresponding ground truth EEG segments are chosen for each of the ten distinct SNR levels (3,611 pairs of ground truth EEG and EMG contaminated EEG for each SNR level), and then all the 10 × 3,611 pairings are combined to form the training set of 36,110 pairs of ground truth EEG and EMG contaminated EEG. The remaining 20% EMG-contaminated EEG segments and their corresponding ground truth EEG segments are also formed (903 pairings of ground truth EEG and EMG contaminated EEG for each SNR level) and combined (10 × 903) to create the test set of 9,030 pairs. Table 2 represents the formation of train and test sets.

Table 2. Formation of train and test sets for experiment B

SNR level(in dB)	Total Number ofGround Truth EEG and EMG Contaminated EEG	80% of Ground Truth EEG and EMG Contaminated EEG	Total Number of Pairs forTrain Set	20% of Ground Truth EEG and EMG Contaminated EEG	Total Number of Pairs for Test Set
-7	4,514	3,611	36,110	903	9,030
-6	4,514	3,611		903	
-5	4,514	3,611		903	
-4	4,514	3,611		903	
-3	4,514	3,611		903	
-2	4,514	3,611		903	
-1	4,514	3,611		903	
0	4,514	3,611		903	
+1	4,514	3,611		903	
+2	4,514	3,611		903	

In experiment A, DL models are trained and evaluated for certain SNR level segments; as a result, they are not capable of performing well if tested with other SNR-level EEG segments. This is the main difference between experiments A and B. Since there is no way to determine the SNR level of the applied input signal in real-world circumstances, models trained as experiment B should be more reliable when evaluated with EMG-contaminated EEG segments having different SNR levels.

In experiment B, all four 1D CNN segmentation networks are trained with and without Deep supervision [36]. It is found that the deep supervision did not improve the model performance, hence we have not reported the results utilizing deep supervision for this experiment. Unlike experiment A, the performance of the trained models is quantified using five performance metrics (average power ratio between five different EEG bands to the whole spectra, relative root mean squared error in the time domain, relative root mean squared error in the frequency domain, the temporal percentage reduction in EMG artifacts, and lastly, the spectral percentage reduction in EMG artifacts.

3.3. Performance Metrics

It is key to quantify the model's performance to ascertain how well it can predict the signal. In addition, identifying and selecting the appropriate performance metrics is crucial. In this regard, to measure the adeptness of the four 1D CNN models quantitatively, the correlation coefficient (CC) in the time domain, the percentage reduction in artifacts in the time and frequency domain, the temporal and spectral relative root mean squared error (RRMSE) is measured using the following formulas which can be found in Equation 5-9 [12, 29]:

$$CC_{temporal} = \frac{Cov(\hat{z},\hat{x})}{\sqrt{Var(\hat{z})Var(\hat{x})}} \quad (5)$$

$$\eta = 100\ (1 - \frac{1-CC_{temporal(after)}}{1-CC_{temporal(before)}}) \quad (6)$$

$$\gamma = 100\ (1 - \frac{1-CC_{spectral(after)}}{1-CC_{spectral(before)}}) \quad (7)$$

$$RRMSE_{temporal} = \frac{RMS(\hat{z}-\hat{x})}{RMS(\hat{x})} \quad (8)$$

$$RRMSE_{spectral} = \frac{RMS(PSD(\hat{z})-PSD(\hat{x}))}{RMS(PSD(\hat{x}))} \quad (9)$$

Where, Cov stands for covariance, Var means the variance, $\hat{x}$ is the normalized ground truth EEG, $\hat{z}$ is the predicted segment, η stands for the temporal percentage reduction in EMG artifacts, γ is the spectral percentage reduction in EMG artifacts, $CC_{temporal(after)}$ is the temporal CC between predicted and ground truth EEG segment, $CC_{temporal(before)}$ is the temporal CC between contaminated and ground truth EEG segment, $CC_{spectral(after)}$ is the frequency domain CC between predicted and ground truth EEG segment, $CC_{spectral(before)}$ represents the frequency domain CC between contaminated and ground truth EEG segment, and PSD is the power spectral density.

In addition to the aforementioned performance metrics, the average power ratio of each EEG frequency band (delta [1-4 Hz], theta [4-8 Hz], alpha [8-13 Hz], beta [13-30 Hz], and gamma [30-80 Hz] bands) to the whole band (1-80 Hz) is also computed and reported for the EMG contaminated EEG, ground truth EEG, and predicted EEG segments.

4. RESULTS AND DISCUSSION

The results of experiments A and B are described and discussed in detail in this section.

4.1. Results of Experiment A

Figure 4 depicts the average temporal correlation coefficient values between predicted denoised EEG segments (after the removal of EMG artifacts) and the ground truth EEG segments for ten distinct SNR values ranging from -7 dB to +2 dB obtained from four different 1D CNN models separately. The RRMSE values in the temporal and spectral domain are also plotted against ten distinct SNR levels in the same figure.

For EMG artifacts removal from EEG, all four 1D CNN models performed very close as is evident from Figure 4 where almost overlapping curves of performance metrics can be seen. Overall, for EMG artifacts removal from noisy EEG, the performance of the DL models improved (higher CC, lower RRMSE value in temporal and spectral domain) with the increment of SNR level and vice versa, which is expected. As the SNR level increases, EMG noise also reduces proportionally and therefore DL models face lesser challenges in developing the non-linear mapping function for predicting denoised EEG segments. In this process, the performance of the models improves for higher SNR levels and vice versa.

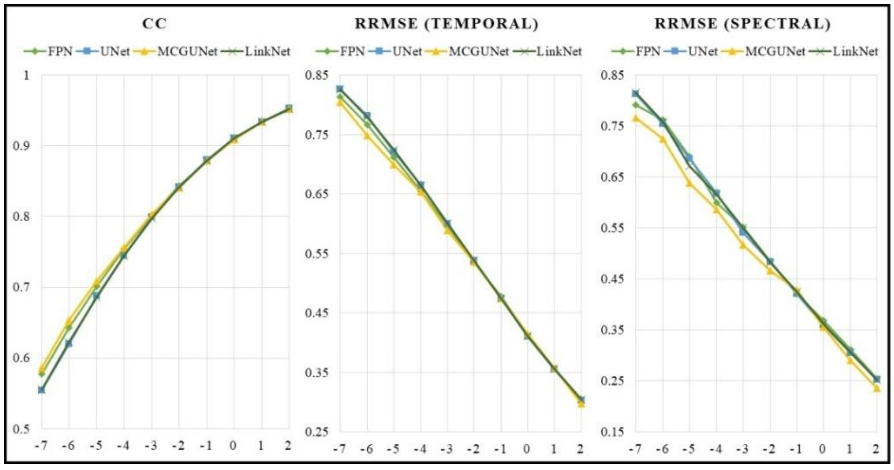

Figure 4. Performance parameters of four 1D CNN models at ten different SNR levels after denoising EMG-contaminated EEG.

4.2. Results of Experiment B

The goal of the four 1D segmentation networks is to remove/reduce EMG artifacts from the EEG segments. To provide a qualitative assessment of the denoising models used, Figure 5(a) shows one EMG-contaminated EEG segment whereas Figure 5(b)–(e) shows EMG artifacts-free EEG (predicted EEG) segments for all four models.

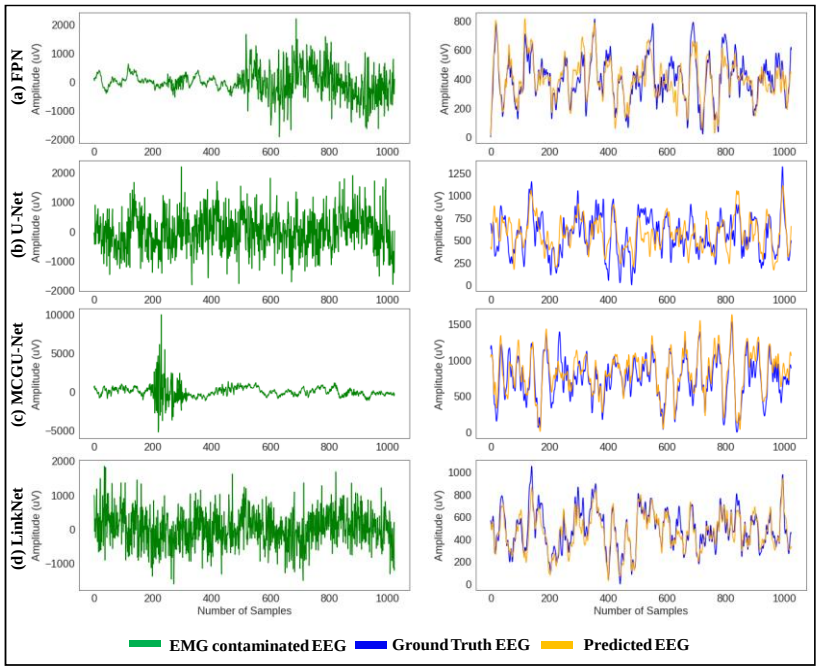

Figure 5. (a) Example EMG contaminated EEG segment; EMG artifacts-free EEG segments predicted by (b) FPN, (c) U-Net, (d) MCGU-Net, and (e) LinkNet networks overlaid with the ground truth EEG.

In Table 3, Temporal and spectral percentage reduction in EMG artifacts, as well as Temporal and spectral RRMSE values are summarized for the prediction of EMG artifacts free EEG segments by the four different 1D CNN models separately. For EMG corrupted EEG segments, the best denoising (elimination of EMG artifacts) performance is generated by the U-Net model. In the time domain, 90.01% reduction in EMG artifacts is found whereas, in the frequency domain, 95.49% EMG artifacts removal is observed while U-Net is utilized. Again, the very same model produced the lowest RRMSE values both in the time and frequency domain (0.10042 and 0.20276, respectively) in comparison with the other three 1D CNN networks. While the U-Net model dominates in producing better denoising performance, LinkNet produced the lowest temporal percentage reduction in EMG artifacts (85.09%) along with the highest temporal RRMSE (0.15681) wheras the FPN model produced lowest spectral percentage reduction in EMG artifacts (91.31%) along with the highest spectral RRMSE (0.31715).

Table 3. Performance parameters of 1D CNN models after denoising EMG-contaminated EEG. The asterisk (*) sign represents the best performing results

Model Name	**Temporal Percentage Reduction in EMG Artifacts (in %)**	**Spectral Percentage Reduction in EMG Artifacts (in %)**	**Temporal RRMSE +/- Std. Deviation**	**Spectral RRMSE +/- Std. Deviation**
FPN [31]	86.31	91.31	0.14131 +/- 0.08200	0.31715 +/- 0.26364
U-Net [32]	90.01*	95.49*	0.10042 +/- 0.07001*	0.20276 +/- 0.14862*
MCGU-Net [33]	89.10	94.13	0.13811 +/- 0.08458	0.28561 +/- 0.23205
LinkNet[34]	85.09	91.88	0.15681 +/- 0.08843	0.30818 +/- 0.18860

Table 4 represents the average power ratios calculated between five different EEG bands (Delta, Theta, Alpha, Beta, Gamma) before and after the elimination of EMG artifacts. The closer value of the average power ratios of different bands compared with ground truth EEG signifies the close resemblance and data fidelity while predicted by the deep learning models. We found that the U-Net model dominates in producing the closest average power ratios for theta, alpha, beta, and gamma-band while compared with the ground truth EEG and for delta band power ratio, MCGU-Net performed best whereas the EMG contaminated EEG produced the worst average power band ratios for all the five bands due to the incorporation of EMG noises, as expected.

Table 4. Average power ratios of five EEG frequency bands before and after the denoising of EMG-contaminated EEG. The asterisk (*) sign represents the best-performing results.

Model/ Method	**Delta**	**Theta**	**Alpha**	**Beta**	**Gamma**
FPN [31]	0.41474	0.5641	0.12416	0.06783	0.0155
U-Net [32]	0.40727	0.55701*	0.12904*	0.07516*	0.01822*
MCGU-Net [33]	0.40725*	0.57707	0.12354	0.06745	0.01351
LinkNet[34]	0.41106	0.56383	0.12619	0.0697	0.01604
EMG contaminated EEG	0.1331	0.10418	0.06205	0.20869	0.55126
Ground Truth EEG	0.40504	0.5429	0.13225	0.08214	0.02146

Due to the temporal complexity and presence of high-frequency components in EMG signals, removing EMG artifacts is always more challenging compared to the removal of other physiological artifacts from EEG recordings [37]. Similar phenomena are also observed in this well-crafted study. However, the findings from this work show that EEG artifact reduction DL models are very dependable owing to the amazing flexibility and strong generalizability of deep learning models. Although the DL-based denoising algorithms need a significant quantity of ground truth EEG data during the training phase, they may be used consistently to remove EMG artifacts from noisy EEG signals after the model has been trained.

The use of a semi-synthetic dataset is also justified by the fact that the presence of ground truth EEG is required for assessing 1D CNN models' performance. In this study, the EMG segments that are linearly mixed with EEG segments were collected from the real-life test subjects rather than producing it artificially which further ensures the efficacy of the proposed models.

RRMSE in the time and frequency domain, as well as CC, have been calculated to assess the efficacy of the four distinct 1D segmentation networks in predicting artifact-free EEG data, as also reported in [29]. Additionally, to measure the effectiveness of DL models, we have included two new performance criteria in this study, namely the percentage decrease in EMG artifacts in

the time and frequency domains separately. We firmly believe that including the three-performance metrics mentioned before with these new two would help standardize the quantitative performance evaluation of DL models to a great extent.

5. CONCLUSIONS

In this paper, four 1D CNN models i.e. FPN, U-Net, MCGU-Net, and LinkNet are utilized to remove EMG artifacts from EEG signal. While using U-Net, the EMG artifacts from EMG-corrupted EEG are decreased by 90.01% and 95.49%, in the time and frequency domains, respectively. The lowest temporal and spectral RRMSE (0.1 and 0.2, respectively) for the denoising of EMG artifacts from contaminated EEG segments are produced by the U-Net model. Also, the same model produced the closest average power ratio for the theta, alpha, beta, and gamma band compared with the ground truth EEG while removing EMG artifacts compared to the other three models. The findings of this work provide a convincing demonstration of the reliability of 1D CNN models in removing EMG artifacts caused by tainted EEG data. Our results demonstrated that DL approaches have a significant ability to remove EMG artifacts from EEG data, even at high noise levels.

ACKNOWLEDGEMENTS

The dataset used in this research work is kindly shared by Zhang et al. [29]. This research is financially supported by Qatar National Research Foundation (QNRF), Grant number NPRP12s-0227-190164 and International Research Collaboration Co-Fund (IRCC) grant: IRCC-2021-001. The statements made herein are solely the responsibility of the authors.

REFERENCES

[1] J. R. Wolpaw, D. J. McFarland, G. W. Neat, and C. A. Forneris, "An EEG-based brain-computer interface for cursor control," Electroencephalography and clinical neurophysiology, vol. 78, no. 3, pp. 252-259, 1991.

[2] Y. Zhang, Y. Guo, P. Yang, W. Chen, and B. Lo, "Epilepsy seizure prediction on EEG using common spatial pattern and convolutional neural network," IEEE journal of biomedical and health informatics, vol. 24, no. 2, pp. 465-474, 2019.

[3] S. Yang, J. M. S. Bornot, K. Wong-Lin, and G. Prasad, "M/EEG-based bio-markers to predict the MCI and Alzheimer's disease: a review from the ML perspective," IEEE Transactions on Biomedical Engineering, vol. 66, no. 10, pp. 2924-2935, 2019.

[4] C. Berka et al., "Real-time analysis of EEG indexes of alertness, cognition, and memory acquired with a wireless EEG headset," International Journal of Human-Computer Interaction, vol. 17, no. 2, pp. 151-170, 2004.

[5] V. Gupta, M. D. Chopda, and R. B. Pachori, "Cross-subject emotion recognition using flexible analytic wavelet transform from EEG signals," IEEE Sensors Journal, vol. 19, no. 6, pp. 2266-2274, 2018.

[6] P. Antonenko, F. Paas, R. Grabner, and T. Van Gog, "Using electroencephalography to measure cognitive load," Educational psychology review, vol. 22, no. 4, pp. 425-438, 2010.

[7] P. Gaur, R. B. Pachori, H. Wang, and G. Prasad, "An automatic subject specific intrinsic mode function selection for enhancing two-class EEG-based motor imagery-brain computer interface," IEEE Sensors Journal, vol. 19, no. 16, pp. 6938-6947, 2019.

[8] A. Rahman et al., "Robust biometric system using session invariant multimodal EEG and keystroke dynamics by the ensemble of self-ONNs," Computers in Biology and Medicine, vol. 142, p. 105238, 2022.

[9] B. W. McMenamin et al., "Validation of ICA-based myogenic artifact correction for scalp and source-localized EEG," Neuroimage, vol. 49, no. 3, pp. 2416-2432, 2010.

[10] A. Flexer, H. Bauer, J. Pripfl, and G. Dorffner, "Using ICA for removal of ocular artifacts in EEG recorded from blind subjects," Neural Networks, vol. 18, no. 7, pp. 998-1005, 2005.

[11] J. Jorge, C. Bouloc, L. Bréchet, C. M. Michel, and R. Gruetter, "Investigating the variability of cardiac pulse artifacts across heartbeats in simultaneous EEG-fMRI recordings: A 7T study," NeuroImage, vol. 191, pp. 21-35, 2019.
[12] M. S. Hossain et al., "Motion Artifacts Correction from Single-Channel EEG and fNIRS Signals Using Novel Wavelet Packet Decomposition in Combination with Canonical Correlation Analysis," Sensors, vol. 22, no. 9, p. 3169, 2022.
[13] B. Somers, T. Francart, and A. Bertrand, "A generic EEG artifact removal algorithm based on the multi-channel Wiener filter," Journal of neural engineering, vol. 15, no. 3, p. 036007, 2018.
[14] A. G. Correa, E. Laciar, H. Patiño, and M. Valentinuzzi, "Artifact removal from EEG signals using adaptive filters in cascade," in Journal of Physics: Conference Series, 2007, vol. 90, no. 1, p. 012081: IOP Publishing.
[15] A. Mert and A. Akan, "Hilbert-Huang transform based hierarchical clustering for EEG denoising," in 21st European Signal Processing Conference (EUSIPCO 2013), 2013, pp. 1-5: IEEE.
[16] M. Marino et al., "Adaptive optimal basis set for BCG artifact removal in simultaneous EEG-fMRI," Scientific reports, vol. 8, no. 1, pp. 1-11, 2018.
[17] M. S. Hossain et al., "Motion Artifacts Correction from EEG and fNIRS Signals using Novel Multiresolution Analysis," IEEE Access, vol. 10, pp. 29760-29777, 2022.
[18] E. Urrestarazu, J. Iriarte, M. Alegre, M. Valencia, C. Viteri, and J. Artieda, "Independent component analysis removing artifacts in ictal recordings," Epilepsia, vol. 45, no. 9, pp. 1071-1078, 2004.
[19] W. De Clercq, A. Vergult, B. Vanrumste, W. Van Paesschen, and S. Van Huffel, "Canonical correlation analysis applied to remove muscle artifacts from the electroencephalogram," IEEE Transactions on Biomedical Engineering, vol. 53, no. 12, pp. 2583-2587, 2006.
[20] K. Zeng, D. Chen, G. Ouyang, L. Wang, X. Liu, and X. Li, "An EEMD-ICA approach to enhancing artifact rejection for noisy multivariate neural data," IEEE transactions on neural systems and rehabilitation engineering, vol. 24, no. 6, pp. 630-638, 2015.
[21] X. Chen, Q. Chen, Y. Zhang, and Z. J. Wang, "A novel EEMD-CCA approach to removing muscle artifacts for pervasive EEG," IEEE Sensors Journal, vol. 19, no. 19, pp. 8420-8431, 2018.
[22] K. T. Sweeney, S. F. McLoone, and T. E. Ward, "The use of ensemble empirical mode decomposition with canonical correlation analysis as a novel artifact removal technique," IEEE transactions on biomedical engineering, vol. 60, no. 1, pp. 97-105, 2012.
[23] A. Krizhevsky, I. Sutskever, and G. E. Hinton, "Imagenet classification with deep convolutional neural networks," Advances in neural information processing systems, vol. 25, 2012.
[24] A. Vaswani et al., "Attention is all you need," Advances in neural information processing systems, vol. 30, 2017.
[25] Z. Tang, C. Li, and S. J. O. Sun, "Single-trial EEG classification of motor imagery using deep convolutional neural networks," Optik, vol. 130, pp. 11-18, 2017.
[26] T.-j. Luo, Y. Fan, L. Chen, G. Guo, and C. Zhou, "EEG signal reconstruction using a generative adversarial network with wasserstein distance and temporal-spatial-frequency loss," Frontiers in neuroinformatics, vol. 14, p. 15, 2020.
[27] N. M. N. Leite, E. T. Pereira, E. C. Gurjao, and L. R. Veloso, "Deep convolutional autoencoder for EEG noise filtering," in 2018 IEEE International Conference on Bioinformatics and Biomedicine (BIBM), 2018, pp. 2605-2612: IEEE.
[28] W. Sun, Y. Su, X. Wu, and X. Wu, "A novel end-to-end 1D-ResCNN model to remove artifact from EEG signals," Neurocomputing, vol. 404, pp. 108-121, 2020.
[29] H. Zhang, M. Zhao, C. Wei, D. Mantini, Z. Li, and Q. Liu, "Eegdenoisenet: A benchmark dataset for deep learning solutions of eeg denoising," Journal of Neural Engineering, vol. 18, no. 5, p. 056057, 2021.
[30] H. Zhang, C. Wei, M. Zhao, Q. Liu, and H. Wu, "A novel convolutional neural network model to remove muscle artifacts from EEG," in ICASSP 2021-2021 IEEE International Conference on Acoustics, Speech and Signal Processing (ICASSP), 2021, pp. 1265-1269: IEEE.
[31] T.-Y. Lin, P. Dollár, R. Girshick, K. He, B. Hariharan, and S. Belongie, "Feature pyramid networks for object detection," in Proceedings of the IEEE conference on computer vision and pattern recognition, 2017, pp. 2117-2125.
[32] O. Ronneberger, P. Fischer, and T. Brox, "U-net: Convolutional networks for biomedical image segmentation," in International Conference on Medical image computing and computer-assisted intervention, 2015, pp. 234-241: Springer.

[33] M. Asadi-Aghbolaghi, R. Azad, M. Fathy, and S. J. a. p. a. Escalera, "Multi-level context gating of embedded collective knowledge for medical image segmentation," 2020.
[34] A. Chaurasia and E. Culurciello, "Linknet: Exploiting encoder representations for efficient semantic segmentation," in 2017 IEEE Visual Communications and Image Processing (VCIP), 2017, pp. 1-4: IEEE.
[35] X. Chen, H. Peng, F. Yu, and K. Wang, "Independent vector analysis applied to remove muscle artifacts in EEG data," IEEE transactions on instrumentation and measurement, vol. 66, no. 7, pp. 1770-1779, 2017.
[36] Q. Zhu, B. Du, B. Turkbey, P. L. Choyke, and P. Yan, "Deeply-supervised CNN for prostate segmentation," in 2017 international joint conference on neural networks (IJCNN), 2017, pp. 178-184: IEEE.
[37] Z.-Q. J. Xu, Y. Zhang, T. Luo, Y. Xiao, and Z. Ma, "Frequency principle: Fourier analysis sheds light on deep neural networks," arXiv preprint arXiv:.06523, 2019.

AUTHORS

Muhammad E. H. Chowdhury received his Ph.D. degree from the University of Nottingham, U.K., in 2014. He worked as a Postdoctoral Research Fellow at the Sir Peter Mansfield Imaging Centre, University of Nottingham. He is currently working as an Assistant Professor with the Department of Electrical Engineering, Qatar University. He has filed several patents and published more than 100 peer-reviewed journal articles, conference papers, and several book chapters. His current research interests include biomedical instrumentation, signal processing, wearable sensors, medical image analysis, machine learning and computer vision, embedded system design, and simultaneous EEG/fMRI. He is currently running several NPRP, UREP, and HSREP grants from Qatar National Research Fund (QNRF) and internal grants (IRCC and HIG) from Qatar University along with academic projects from HBKU and HMC. He has been involved in EPSRC, ISIF, and EPSRC-ACC grants along with different national and international projects during his tenure at the University of Nottingham. He is a Senior Member of IEEE, and a member of British Radiology, ISMRM, and HBM. He is serving as an Associate Editor for IEEE Access and a Topic Editor and Review Editor for Frontiers in Neuroscience. He has recently won the COVID-19 Dataset Award, AHS Award from HMC, and National AI Competition awards for his contribution to the fight against COVID-19.

Md Shafayet Hossain received his B.Sc. in Electrical and Electronic Engineering from the Islamic University of Technology (IUT), Dhaka, Bangladesh. Currently, he is pursuing an M.Sc. in Universiti Kebangsaan Malaysia (UKM) focusing on the removal/reduction of motion artifacts from physiological signals (especially from EEG signals) using traditional signal processing and machine learning-based models. Mr. Shafayet is an active member of Qatar University Machine Learning Group (initiated and supervised by Dr. Muhammad E. H. Chowdhury) from October 2020 to the present. He also worked as a Research Assistant at Qatar University from May 2021 to September 2021. He joined the Department of EEE of Bangladesh University of Business and Technology, Dhaka, Bangladesh as a Lecturer in 2015 and is currently on study leave. His research interests include biomedical signal processing, machine learning & deep learning, bio-sensor design, green energy harvesting, and power electronics.

Sakib Mahmud received his Bachelor of Science (BSc.) degree in Electrical Engineering with an Honours from Qatar University (QU) in June 2020 and currently pursuing his Master of Science (MSc.) in Electrical Engineering from the same department. As an undergraduate student, he received the Dean's Award for six semesters during 2016-2019. As an undergraduate student at QU, He has been a part of two UREP projects funded by the QNRF. Upon graduation, he joined QU's master's program to pursue a postgraduate degree in electrical engineering and work as a Graduate Research Assistant (GRA) at the same time, under the same department. As a GRA, and a member of QU Machine Learning Group, he was hired in two QNRF funder NPRP grants and three High Impact grant from QU. Currently he is hired in a High Impact grant funded by QU. Apart from his research work, he has been an Electrical Engineering Intern in the Electrical Consultant Group (E.C.G.) Qatar Branch, Data Science Intern in Data Glacier and has been selected as an Artificial Intelligence (AI) Intern in AI Ready Academy, a joint training program for

Machine Learning and Data Science by Microsoft and ZAKA, among 2000 competitive applicants around the Middle East and North Africa (MENA) region, He has expertise in Electronics Circuitry design, 3D Modeling, Biomedical Signal and Image Processing, Computer Vision, Machine and Deep Learning, and Data Analytics and Visualization in various platforms. Currently, he has published 10 articles in peer reviewed Journals, one conference paper and one patent.

Amith Khandakar received the B.Sc. degree in electronics and telecommunication engineering from North South University, Bangladesh, and the master's degree in computing (networking concentration) from Qatar University, in 2014. He graduated as the Valedictorian (President Gold Medal Recipient) of North South University. He is an IEEE Senior Member. He is also a certified Project Management Professional and the Cisco Certified Network Administrator. He has 2 patents and published around 60 peer-reviewed journal articles, conference papers, and four book chapters. His current research interests include biomedical instrumentation, wearable sensors, medical image analysis, machine learning and Engineering Education. He is also running UREP grants from QNRF and internal grants from Qatar University.